RESEARCH ARTICLE

Potential biomarkers for ischemic heart damage identified in mitochondrial proteins by comparative proteomics

Nari Kim, Youngsuk Lee, Hyungkyu Kim, Hyun Joo, Jae Boum Youm, Won Sun Park, Mohamad Warda, Dang Van Cuong and Jin Han

Mitochondrial Signaling Laboratory, Department of Physiology and Biophysics, College of Medicine, Cardiovascular and Metabolic Diseases Research Center, Biohealth Products Research Center, Inje University, Busan, Korea

We used proteomics to detect regional differences in protein expression levels from mitochondrial fractions of control, ischemia–reperfusion (IR), and ischemic preconditioned (IPC) rabbit hearts. Using 2-DE, we identified 25 mitochondrial proteins that were differentially expressed in the IR heart compared with the control and IPC hearts. For three of the spots, the expression patterns were confirmed by Western blotting analysis. These proteins included 3-hydroxybutyrate dehydrogenase, prohibitin, 2-oxoglutarate dehydrogenase, adenosine triphosphate synthases, the reduced form of nicotinamide adenine dinucleotide (NADH) oxidoreductase, translation elongation factor, actin alpha, malate dehydrogenase, NADH dehydrogenase, pyruvate dehydrogenase and the voltage-dependent anion channel. Interestingly, most of these proteins are associated with the mitochondrial respiratory chain and energy metabolism. The successful use of multiple techniques, including 2-DE, MALDI-TOF-MS and Western blotting analysis demonstrates that proteomic analysis provides appropriate means for identifying cardiac markers for detection of ischemia-induced cardiac injury.

Received: April 30, 2005
Revised: October 18, 2005
Accepted: October 23, 2005

Keywords:
Cardiac marker / Ischemia–reperfusion / Ischemic preconditioning / MALDI-TOF-MS / Mitochondria / 2-DE

Correspondence: Dr. Jin Han, Mitochondrial Signaling Laboratory, Department of Physiology and Biophysics, College of Medicine, Cardiovascular and Metabolic Disease Center, Biohealth Products Research Center, Inje University, 633-165 Gaegeum-Dong, Busanjin-Gu, Busan 614-735, Korea
E-mail: phyhanj@ijnc.inje.ac.kr
Fax: +82-51-894-5714

Abbreviations: ATP, adenosine triphosphate; **DRP1**, dynamin-related protein 1; **IPC**, ischemic preconditioning; **IR**, ischemia-reperfusion; **LDH**, lactate dehydrogenase; **MDH**, malate dehydrogenase; **MIB**, mitochondrial isolation buffer; **NADH**, the reduced form of nicotinamide adenine dinucleotide; **OGDH**, 2-oxoglutarate dehydrogenase; **OMM**, outer mitochondrial membrane; **Rsp-chain**, respiratory chain; **TEF**, translation elongation factor; **TTC**, 2,3,5-triphenyl tetrazolium chloride; **VDAC**, voltage-dependent anion channel

1 Introduction

The occurrence of ischemic heart disease along with its associated complications remains the largest cause of death in Western societies [1]. Understanding the cellular mechanism of ischemia–reperfusion (IR) injury is important for reducing cardiac-related morbidity and mortality [2]. Reperfusion of the ischemic myocardium results in widespread lipid and protein oxidative modifications, mitochondrial injury, and tissue apoptosis and necrosis, which can lead to death [3–6]. Ischemic preconditioning (IPC) is defined as a short period of myocardial IR that decreases subsequent lethal IR injury [7–9] and is the most powerful mechanism known for limiting cardiac infarction [9, 10]. However, the mechanisms by which IPC protects the myocardium against IR-induced injury are

still not fully understood. Many studies suggest that substances released during the short preconditioning period of ischemia activate a complex intracellular signaling cascade, which converges on mitochondrial end-effectors, including the mitochondrial potassium channels and the mitochondrial permeability transition pore [11–13].

Mitochondrial mutation and dysfunction have been implicated in numerous diseases, including heart disease, myocardial preconditioning and IR, and neurological diseases [14–16]. The rapidly emerging field of proteomics can now provide a powerful suite of techniques for the identification and characterization of mitochondrial proteins involved in these processes.

Here, we demonstrated the use of proteomics for detection of regional differences of protein expression levels in mitochondrial fractions of control, IR, and IPC hearts.

2 Materials and methods

2.1 Materials

Acrylamide, methylene *bis*-acrylamide, glycine, Tris, urea, glycerol, CHAPS, thiourea, bromophenol blue, 2,3,5-triphenyl tetrazolium chloride (TTC), and Percoll solution were purchased from Sigma (St. Louis, MO, USA). TEMED, iodoacetamide, ammonium persulfate, DTT, and SDS were obtained from Merck (Darmstadt, Germany). IPG strips, IPG buffer, Destreak rehydration solution, and the 2-D Quant kit were purchased from Amersham Biosciences (Uppsala, Sweden). Anti-rabbit, -mouse,-goat IgG antibodies and anti-voltage-dependent anion channel (VDAC) antibody were obtained from Sigma. Anti-prohibitin antibody was supplied by Abcam (Cambridge, UK). Anti-ATP synthase beta subunit antibody was from Becton Dickinson (San Jose, CA, USA). The 1-DE kit and membrane transfer kit were from Hoefer (San Francisco, CA, USA). Immobilon-P membranes were purchased from Millipore (Bedford, MA, USA). ECL Western blotting detection kit was from Amersham Biosciences (Buckinghamshire, UK). All other reagents used were of analytical grade.

2.2 Langendorff perfusion of isolated rabbit hearts

The rabbits were anesthetized with sodium pentobarbital (1 mg/kg) and heparin (300 IU/mL/kg) via an ear vein. The hearts were rapidly excised and placed in cold bicarbonate buffer. The aorta was cannulated with a glass cannula and perfused in a non-recirculating apparatus containing a heart chamber at 12 mL/min with bicarbonate buffer equilibrated with 95% O_2/5% CO_2 at 37°C. The bicarbonate buffer contained (in mM): 118.5 mM NaCl, 3.1 mM KCl, 1.18 mM KH_2PO_4, 1.2 mM $MgCl_2$, 25.0 mM $NaHCO_3$, 1.4 mM $CaCl_2$, and 10.0 mM glucose [17]. We prepared IPC and IR cardiac tissues according to the perfusion protocols summarized in Fig. 1A.

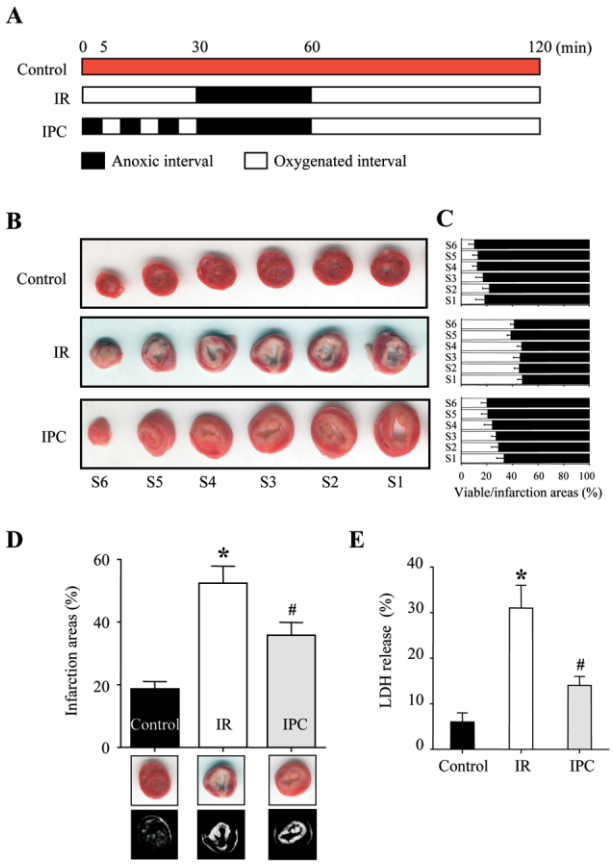

Figure 1. Experimental protocols and measurements of infarction size and LDH release. (A) Experimental protocols. Eighteen rabbit hearts were randomly divided into three equal groups: control groups, ischemia–reperfusion (IR) and ischemic preconditioning (IPC). Hearts were equilibrated in a bath for at least 20 min before application of any of the protocols. Excluding control group, all hearts were made anoxic for 30 min (black area). IR group was exposed to 30-min anoxia alone. In the absence of oxygen, hearts underwent IPC alone. (B) Images of the cross-sectioned heart slices, from slice 1 (base area of heart) to slice 6 (apex of heart). Infarction size expressed as percentage of area at risk. Right panels presented the percentage of infarction (white column) and viable (black column) area in each slice that were analyzed in control, IR, and IPC, respectively. (C) Infarction size as a percentage of totals of six slices from each heart of control, IR, and IPC. Upper images show the representative slices in each condition. Grey-converted images in which pale areas from original one are replaced by white color (lower panel). (D) Lactate dehydrogenase (LDH) release of rabbit hearts 60 min after a 30-min anoxic insult in control, IPC, and IR. Preconditioned hearts showed significantly lower release of LDH on anoxia compared to IR-treated heart. The IR hearts were exposed to the 30-min anoxia only. Data are presented as means ± SEM. $^*p < 0.05$ as compared with control. $^{\#}p < 0.05$ as compared with IR.

Eighteen isolated rabbit hearts were randomly divided equally into three groups (Control, IR and IPC groups, six animals each), and perfused using a modified Langendorff model [18, 19].

Control type heart model was continuously perfused with bicarbonate buffer solution for 140 min including 20-min stabilization period. Inherent to IPC model is the variability in the methods used to simulate ischemia. In the present study, ischemia was simulated by anoxia, which was achieved by substitution of nitrogen for oxygen. IPC type heart model was perfused for 20 min with bicarbonate buffer solution for stabilization. To simulate preconditioning (brief initial preconditioning anoxia), isolated hearts were followed by 5-min perfusion with ischemia solution containing 140 mM NaCl, 8 mM KCl, 0.5 mM $MgCl_2$, 1.8 mM $CaCl_2$ and 10.0 mM deoxyglucose, HEPES, 5.0 pH 6.0 adjusted by NaOH and equilibrated with 100% N_2 at 135~140 mmHg and reperfused for 5 min with bicarbonate buffer solution (ischemia preconditioning). These ischemia-reperfusion periods were repeated twice and then long-term ischemia treatment for 30 min was followed by 60-min reperfusion (second sustained anoxia). Although many studies use duration of anoxia up to 90 min, 30 min has been used in human models [20, 21]. This anoxic period may result in a reversible injury without cell death. Similarly to preconditioning in human models, in this study, prior anoxic preconditioning lessened the injury by 30-min anoxia. Our current findings resemble our previous investigation on heart slices [7] as well as other *in vivo* study [22]. The data provided an important insight by indicating that isolated heart can also be preconditioned. Moreover, the data showed that preconditioning-induced cardioprotective mechanism might be exerted, at least in part, at the level of cardiac myocytes *in vivo*. The use of this heart model for preconditioning and a protocol identical to that employed in preconditioning of *in vivo* experiments would facilitate cellular characterization of this phenomenon and enable quantitative determination of the extent of cardioprotection by preconditioning.

In IR type heart model, isolated hearts were perfused with bicarbonate solution for 60 min. This was followed by direct perfusion with ischemia solution for 30 min and then re-perfused with bicarbonate buffer solution (normoxic perfusion).

2.3 TTC staining

Six rabbits from each group were used to calculate the infarction ratio. In brief, after perfusion treatments (control, IPC, or IR) by Langendorff system, the hearts were sliced into six sections parallel to the atrioventricular groove. The slices were incubated in a TTC solution prepared in phosphate buffer pH 7.4 for 30 min at 37°C [23]. The TTC in viable myocardium was converted by lactate dehydrogenase isoenzymes (LDH, Sigma) to form a red formazan pigment that stains tissue with dark red [24]. The infarct area that did not take the TTC stain remained pale in color.

2.4 Statistical analysis of infarct size

All data are presented as means ± SEM. Statistical analysis was performed by two-way repeated-measures analysis of variance (ANOVA, SuperAnova, Abacus Concepts; Berkeley, CA, USA) for time and treatment (experimental group) effects. If an overall significance was found among the groups, a comparison was done using Student's unpaired *t* test. The differences were considered significant when $p < 0.05$.

2.5 Measurement of LDH release

For the measurement of LDH release, hearts were homogenized in 2 mL of distilled water and the tissue homogenate was centrifuged at $2000 \times g$ at 4°C for 5 min. The pellet was discarded and the supernatant was collected. LDH activity was determined in the supernatant and incubation medium using an LDH assay kit (Asan Pharm., Kyunggee-do, Korea). Final values were expressed as a percentage of the total LDH released from heart slices [25].

2.6 Preparation of myocardial mitochondria

The preparation of highly pure mitochondria is a crucial step for the study of mitochondrial proteins. The mitochondrial sample was prepared according to the methods of Ulrich and Roland [26]. Briefly, cardiac tissues were manually homogenized, using medium fitting glass-teflon Potter-Elvehjem homogenizer in mitochondrial isolation buffer (MIB) that contained 50 mM sucrose, 200 mM mannitol, 5 mM potassium phosphate, 1 mM EGTA, 5 mM MOPS, and 0.1% BSA plus protease inhibitor cocktail at pH 7.4. The resultant homogenate was centrifuged at $1500 \times g$ for 5 min at 4°C. Afterward, the supernatant was centrifuged again at $10\,000 \times g$ for 10 min. The mitochondria-enriched pellet was gently homogenized in 5 mL of 19% Percoll in MIB for the second purification on a Percoll density gradient. This gradient was prepared by careful stepwise layering of 3 mL of 52, 3 mL of 42, and 3 mL of 31% Percoll solutions in a centrifuge tube. Crude mitochondrial fractions (containing 19% Percoll solution) were layered on top of the Percoll density gradient and centrifuged at $100\,000 \times g$ for 1 h at 4°C. The major band at the interface of the 52 and 42% Percoll solutions was collected, diluted with three volumes of MIB, and centrifuged twice at $15\,000 \times g$ for 10 min. The purity of the mitochondria was assessed using an electron microscope (JEOL 1200 EX2, Japan), which showed that mitochondria of a high purity were obtained [27].

2.7 The 2-DE of mitochondrial proteins

The mitochondrial pellet was dissolved in lysis buffer (7 M urea, 2 M thiourea, 4% CHAPS, 40 mM Tris base, 1% DTT, 0.5% IPG buffer, 0.5% Triton X-114, and protease inhibitor cocktail) and kept at room temperature for 1 h. The

protein content was assayed using a 2-D Quant kit (GE Healthcare), and 2-DE was performed as described by Berkelman and Stenstedt [28].

A 24-cm (pH 3–10) IPG strip was rehydrated overnight at 30 V in 450 μL of an IEF solution that contained approximately 500 μg of the solubilized mitochondrial proteins. IEF was carried out at 60 000 V/h at 20°C as follows: 500 V for 1 h, 1000 V for 1 h, and finally 8000 V incremented to 60 000 V/h. The IPG strips were placed in 10 mL of an equilibration solution (50 mM Tris-HCl, pH 8.8, containing 6 M urea, 30% glycerol, 2% SDS, and bromophenol blue) that contained 1% DTT v/v during the first equilibration step and 2.5% iodoacetamide v/v during the second equilibration step (15 min per equilibration step). The 2-D separation was performed using the Ettan DALT twelve system (Amersham). The IPG strips were loaded onto a 12.5% SDS-PAGE gel, running buffer (25 mM Tris, 192 mM glycine, 3.5 mM SDS at pH 8.3) was added, and a constant current (5 W/gel) was applied for 6 h. The gels were then stained with silver nitrate. The stained gels were scanned on a flatbed scanner and the images were analyzed using commercially available software (Image Master 2D Platinum; Amersham Bioscience, USA).

2.8 Protein identification

For MS fingerprinting, the stained portions of the 2-D gel (see Fig. 2) were excised and then digested with trypsin as described by Rosenfeld *et al*. [29]. Isolated protein spots were destained with 100 mM sodium thiosulfate and 30 mM potassium ferricyanide. After washing with 50% ACN, the gel fragments were dried in a vacuum centrifuge. The dried gel fragments were rehydrated in 20 μL of 25 mM NH_4HCO_3 that contained 0.5 μg of sequencing-grade trypsin (Promega, Madison, WI, USA), and were incubated overnight at 37°C. The remaining peptides were extracted twice with 30 μL of 50 mM NH_4HCO_3:ACN (1:1) mixture. The extracts were evaporated in a vacuum centrifuge for further drying. Aliquots of the peptide-containing samples were applied to a target disk and were left to evaporate. Spectra were obtained using a Voyager DE PRO MALDI-MS (Applied Biosystems, Foster City, CA, USA). Protein databases were searched with MASCOT using monoisotope peaks. A mass tolerance within 50 ppm was allowed initially, after which a recalibration was performed using the list of proteins that were obtained within the tolerance of 20 ppm.

2.9 Western blot analysis

Twenty micrograms of mitochondrial protein from each heart were separated by 10% SDS-PAGE. The proteins were transferred to Immobilon-P membranes, which were blocked overnight in TBS (20 mM Tris and 150 mM NaCl, pH 8.0) containing 5% nonfat dry milk and then probed with antibodies of VDAC, prohibitin, pyruvate dehydrogenase, ATP synthase β-subunit at a dilution of 1 μg/mL for 1 h at room temperature. The membranes were incubated with horseradish peroxidase-conjugated secondary antibody at a dilution of 1:2000 for 1 h at room temperature. Immunoreactivity was visualized with an ECL Western blotting detection kit (Amersham Biosciences) under LAS 3000 image detector (Fuji film, Miyagi, Japan).

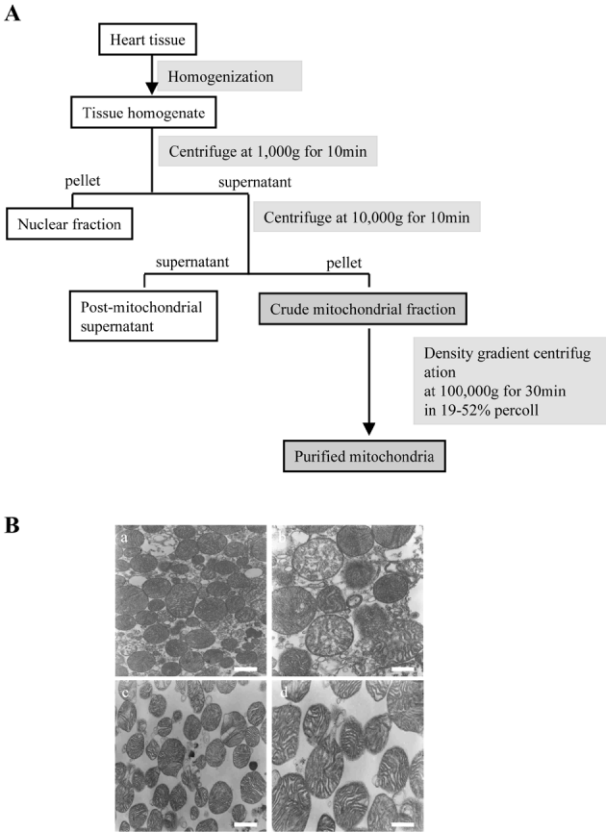

Figure 2. Generalized flow chart for the preparation of intact mitochondria (A). Electron micrographs of isolated rabbit cardiac mitochondria by Percoll density gradient centrifugation (B). The a and b, crude mitochondrial fraction; c and d, purified mitochondria.

3 Results and discussion

3.1 Results

3.1.1 Infarct size and LDH release

Histochemical staining with TTC showed clear evidence of myocardial infarction. The results of TTC perfusion showed two colors and a distinctive pattern. Viable tissues (dominant in normal and IPC hearts) appeared deep red, and the regions of infarction remained pale. Representative images of heart sections from each experimental group are shown in Fig. 1B. The IR group rabbits had large unstained areas located in the anterior and lateral part of the left ventricular

(LV) wall. IPC reduced heart damage by reducing infract size from 52.4 ± 5.5 (n = 6) to 35.8 ± 4.1% (n = 6). Fig. 1C and D summarize the infarct size in each group. For further evaluation of the cardioprotective effect of IPC on simulated myocardial ischemia model, the effects of IPC on LDH release were determined at the end of 60-min post-anoxia in pretreated hearts with anoxia. In Fig. 1E, the LDH release in control group was 6.3 ± 2.5% (n = 6). In IR group, the LDH release was significantly increased compared with control (31.4 ± 5.2%, n = 6). Pretreatment of the hearts with three successive 5-min anoxic intervals resulted in a significant reduction in the LDH release (14.7 ± 2.2%, n = 6).

3.1.2 Mitochondrial isolation and electron microscopy

Percoll density gradient technique takes an advantage for subcellular organelles fractionation depending on their density, which is a function of their lipid: protein ratios. So far, this method has provided an optimum recovery of active and pure myocardial mitochondria [26]. Even after a single-step gradient, the brownish mitochondria-containing fractions can be separated easily by Percoll density differences (Fig. 2A). A representative electron micrograph of the isolated mitochondria is shown in Fig. 2B.

3.1.3 Changes in mitochondrial protein expression

Fractions of heart mitochondrial proteins from control, IPC, and IR rabbits were prepared as described in Section 2.6. For comparison of the expression levels of mitochondrial proteins in control, IPC, and IR samples, we performed 2-DE. Based on an automated spot-counting algorithm provided by Image Master 2D Platinum, means of 342.2 ± 3.5, 353.5 ± 6.2, and 327.1 ± 3.7 protein spots were detected from the control, IPC, and IR groups, respectively. The expression patterns of the mitochondrial proteins are shown in Fig. 3 (A, Control, B, IR, C, IPC). The mitochondrial proteins from three different cardiac samples were distributed in the region of pI 4–9 and had molecular weights between 30 and 150 kDa. The changes in protein production levels were also determined. Twenty-three proteins (approximately 8% of total) were found to have different quantities in the IR group, 13 spots increased and 10 spots decreased, compared with the spots from control cardiac mitochondria. Additionally 2 constant spots were selected for comparison with changed spots (Fig. 4A and B). Finally, the 23 spots (spots in Fig. 4) that changed over 22% in level during IR and 2 constant spots were selected and further identified.

3.1.4 Protein identification

Twenty-five spots in the 2-DE gels of the IR cardiac mitochondria were isolated (Fig. 4) and subjected to MALDI-TOF-MS. The peptides mass peaks were compared with those in the NCBI database (Fig. 5). The protein data

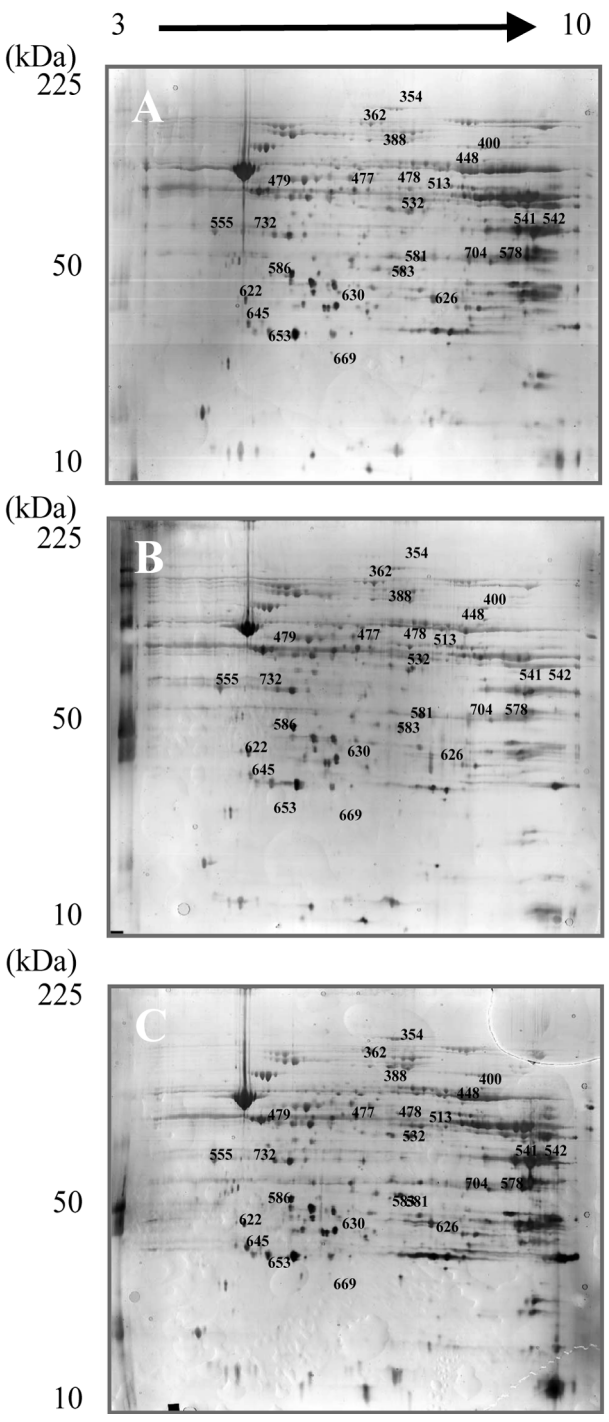

Figure 3. 2-DE analysis of mitochondrial proteins in rabbit heart tissue. Samples of control, ischemic preconditioned, and ischemia–reperfusion mitochondria are shown. (A) Control, (B) ischemia–reperfusion, (C) ischemic preconditioned. Twenty-three significantly changed spots and two constant spots were selected.

descriptions are listed in Table 1. Of the 25 protein spots, 22 were identified and categorized into seven groups: TCA-cycle, α-keto acid dehydrogenases (pyruvate dehydrogenase

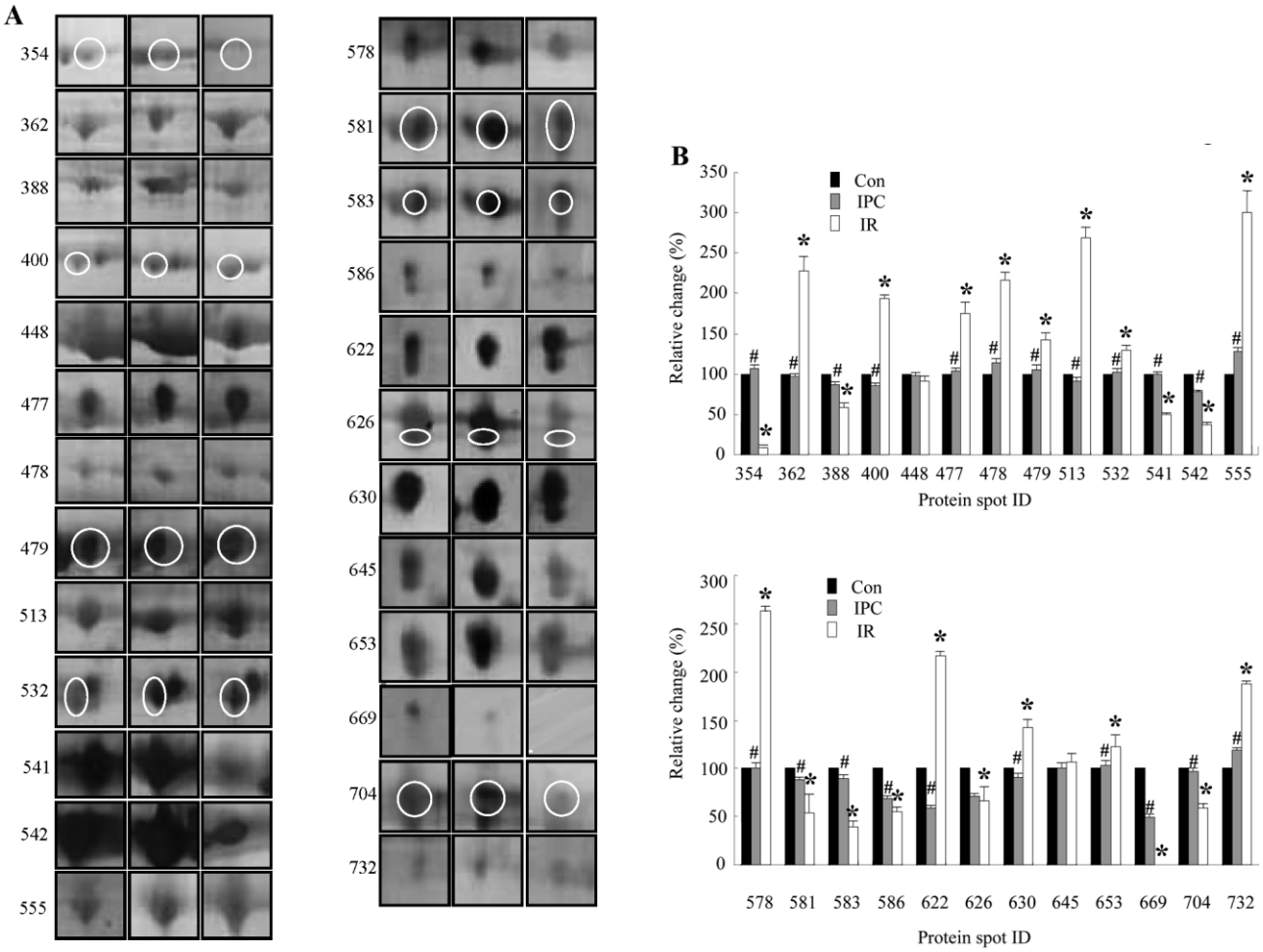

Figure 4. (A) Enlarged 2-DE images showing the over and under expression of proteins in IR mitochondrial samples (C) compared with expression in IPC (B) and control (A) samples. (B) Histogram of different mitochondrial protein production levels in control, IPC, IR heart, respectively (% to control) $^{*}p < 0.05$ *vs.* control, $^{\#}p < 0.05$ *vs.* IR.

complex), respiratory chain (Rsp-chain), mitochondria membrane channel proteins, β-oxidation, proliferation and skeletal protein.

Three TCA-cycle and one α-keto acid dehydrogenases related proteins were identified as 2-oxoglutarate dehydrogenase (OGDH, spot no. 354), two subunits malate dehydrogenase (MDH, spot no. 541, 542) and pyruvate dehydrogenase E1-beta subunit (spot no. 732). Seven Rsp-chain related proteins were identified as ATP synthase F1 α-subunit (ATPsyn-F1-α, spot no. 448), NADH ubiquinone oxidoreductase (spot no. 477), NADH dehydrogenase 1α (spot no. 532), 24-kDa subunit of complex I, NADH dehydrogenase subunit (spot no. 630), NADH dehydrogenase (ubiquinone) Fe-S protein (spot no. 645), ATP synthase, H^+ transporting, mitochondrial F_O complex (spot no. 653), and Rieske iron sulfur protein, complex III-related protein (spot no. 626).

One mitochondria membrane channel protein was identified, VDAC (spot no. 704).

Four proteins that related to β-oxidation and ketone body formation were identified. They were long chain acyl-CoA dehydrogenase (spot no. 513), 3-hydroxybutyrate dehydrogenase (spot no. 578) and enoyl CoA hydratase (ECH, spot no. 581, 583).

Three proliferation-related proteins were identified, namely mitofilin (spot no. 362), translation elongation factor (TEF, spot no. 478), and prohibitin (spot no. 586).

Three skeletal protein were identified, actin alpha (spot no. 479), tropomyosin (spot no. 555) and myosin, light polypeptide (spot no. 622).

In Table 2 different protein expression ratios were presented. The expression of three TCA-cycle proteins, OGDH and MDH decreased relatively (over 51%) compared to control and IPC hearts. One α-keto acid dehydrogenases complex enzyme, pyruvate dehydrogenase, increased 87% compared to control hearts. Rsp-chain related proteins showed various patterns, respiratory chain complex 1 proteins, NADH dehydrogenase, NADH oxidoreductase, NADH

Table 1. Proteins identified from changes in the spots representing the levels of mitochondrial protein in IR samples versus those in IPC and control samples[a)]

Category	Spot no.	gi	Protein	Pep	Score	M_r*	p*I**
TCA-cycle	354	1352618	2-Oxoglutarate dehydrogenase	15	82	113 403	6.62
Proliferation	362	5803115	Mitofilin	16	93	83 616	6.08
RSP-chain	448	6680748	ATP synthase, F1.a	19	148	59 716	9.22
RSP-chain	477	833783	NADH Ubiquinone oxidoreductase	14	102	48 915	5.85
Proliferation	478	2119917	Translation elongation factor	14	119	49 376	6.75
Skeletal protein	479	627834	Actin alpha	14	111	41 758	5.23
β-Oxidation	513	47522692	Long-chain acyl-CoA dehydrogenase	20	267	48326	6.96
RSP-chain	532	13195624	NADH dehydrogenase alpha 10	2	199	40 578	6.52
TCA-cycle	541	42476181	Malate dehydrogenase	12	89	35 661	8.93
TCA-cycle	542	387422	Malate dehydrogenase	12	93	35 588	8.93
Skeletal protein	555	230768	Tropomyosin	17	154	32 661	4.69
β-Oxidation	578	55742813	3-Hydroxybutyrate dehydrogenase	9	132	38 708	9.01
β-Oxidation	581	15080016	Enoyl-coenzyme A hydratase(ECH1)	2	185	35 793	8.16
β-Oxidation	583	15080016	Enoyl-coenzyme A hydratase(ECH1)	2	203	35 793	8.16
Proliferation	586	49456373	Prohibitin	9	174	29 871	5.57
Skeletal protein	622	33563264	Myosin, light polypeptide 3	6	84	22 521	5.03
RSP-chain	626	39939340	Rieske iron sulfur protein	2	175	22 295	7.39
RSP-chain	630	3123721	NADH dehydrogenase subunit 24-kDa	5	71	25 699	7.07
RSP-chain	645	27807359	NADH dehydrogenase (ubiquinon) Fe-S protein	10	203	23 881	6.45
RSP-chain	653	5453559	ATP synthase, F0 subunit	2	100	18 480	5.21
Channel protein	704	59858401	VDAC-2	8	121	32 113	7.48
α-Keto acid dehydrogenases	732	190792	Pyruvate dehydrogenase E1-beta subunit	2	170	39 194	6.2

a) The p*I* and mass values were obtained from the MASCOT database. Individual scores indicate extensive homology. (RSP-chain, respiratory-chain, gi, Gene bank ID, Pep, matched peptide number, score, MASCOT score) * calculated value.

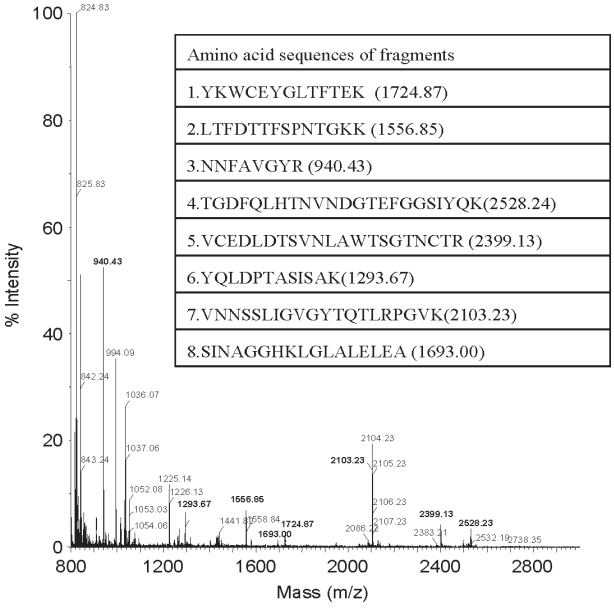

Figure 5. MALDI-TOF spectra of VDAC protein isolated from a 2-D gel of rabbit heart mitochondria. The representative peak spectra from 22 total peaks. Eight matched peptides were labeled bold on the peaks.

dehydrogenase 24-kDa subunit, and NADH dehydrogenase Fe-S protein, increased in IR. However, ATP synthase and complex V-related proteins did not significantly changed. In contrast, Rieske iron sulfur protein and complex III-related protein decreased significantly. For VDAC, a mitochondrial membrane channel protein, expression decreased by 42%. β-Oxidation enzyme proteins, long-chain acyl-CoA dehydrogenase and 3-hydroxybutyrate dehydrogenase increased remarkably but enoyl-CoA hydratase decreased. Proliferation proteins also showed remarkable changes, *e.g.* mitofillin and translation elongation factor increased and prohibitin decreased significantly. All skeletal proteins, α-actin (no. 479), tropomyosin (no. 555) and myosin (no. 622), increased by 43, 200 and 116%, respectively.

3.1.5 Western blot analysis

Three interesting protein spots were selected and subjected to Western blot analysis. These were VDAC, prohibitin and ATP synthase. The Western blot data analysis (Fig. 6) confirmed the 2-DE gel image data. Compared with the control group, in the IR-treated hearts, the levels of VDAC protein (Fig. 6B) and prohibitin protein (Fig. 6C) decreased relatively, whereas ATP synthase (Fig. 6D) showed no significant change.

Table 2. Mitochondrial protein expression changes in IR and IPC hearts compared to control[a)]

Protein	con	IPC		IR	
β-Oxidation					
Long-chain acyl-CoA dehydrogenase	100	#90	±5.7	*269	±4.4
3-Hydroxybutyrate dehydrogenase	100	#100	±1.4	*263	±5.5
Enoyl-coenzyme A hydratase(ECH1)-like protein	100	#88	±5.7	*54	±6.0
Enoyl-coenzyme A hydratase(ECH1)-like protein	100	#90	±3.2	*39	±4.0
Channel protein					
VDAC-2	100	#97	±3.4	*58	±4.6
α-Keto acids dehydrogenases					
Pyruvate dehydrogenase E1-beta subunit	100	#119	±5.7	*187	±6.1
Proliferation					
Inner membrane protein, mitochondrial, mitofilin	100	#97	±2.4	*228	±8.0
Translation elongation factor	100	#113	±3.5	*217	±4.3
Prohibitin	100	#69	±2.5	*56	± 6.4
Rsp-chain					
ATP synthase, mitochondrial F1 complex, alpha subunit	100	98	±2.5	91	± 6.1
NADH ubiquinone oxidoreductase	100	#104	±2.3	*175	± 8.0
NADH dehydrogenase 1 alpha 10	100	#102	±3.8	*130	± 4.4
Rieske iron sulfur protein, complex III related protein	100	#71	±3.4	*66	± 6.2
24-kDa subunit of complex I, NADH dehydrogenase subunit	100	#90	±2.3	*142	± 9.8
NADH dehydrogenase (ubiquinon) Fe-S protein	100	100	±2.7	107	± 8.0
ATP synthase, H^+ transporting, mitochondrial F0 complex	100	#102	±4.6	*122	± 8.1
Skeletal protein					
Actin alpha	100	#106	± .2	*143	± 6.1
Tropomyosin	100	#128	±3.5	*300	± 8.9
Myosin, light polypeptide 3	100	#58	±5.2	*216	± 4.5
TCA-cycle					
2-Oxoglutarate dehydrogenase	100	#106	±4.3	*8	± 3.2
Malate dehydrogenase	100	#100	±3.2	*49	± 4.0
Malate dehydrogenase	100	#78	±2.3	*37	± 8.1

a) % Difference from control, mean ± SEM. $*p < 0.05$ *vs.* control, $^{\#}p < 0.05$ *vs.* IR.

3.2 Discussion

3.2.1 General remarks

Mitochondria, the small powerhouse of the cell, are the major contributors in many cellular as well as extracellular regulatory functions that affect the survival and differentiations of living organisms. Although the primary function of mitochondria is to convert organic materials into cellular energy in the form of ATP, mitochondria play an important role in many important metabolic tasks, such as cellular proliferation, regulation of the cellular redox state, fatty acid oxidation, urea cycle, heme and steroid synthesis and heat production. Mitochondrial functional and/or structural alterations proved to have very deleterious effects on cellular level. The mitochondrial permeability transition is believed to be involved in the suicidal process of apoptosis, or programmed cell death. Moreover, there are hints that mitochondrial dysfunction underlies many forms of diseases [30–36]. Primary mitochondrial diseases, however, are relatively rare, probably because major defects in the Krebs cycle or the respiratory chain are incompatible with life and many affected embryos die at an early stage. Nevertheless, about 150 different types of hereditary mitochondrial defects have been reported, and mitochondria play an important role in several common conditions.

Wide varieties of individual defects have been described affecting one or more of the respiratory chain redox carriers [37–40]. The tissues, which rely most extensively on aerobic metabolism are most severely affected, thus patients commonly present with myopathy or encephalopathy [37], or both. Lactic acidosis [41], muscular weakness, deafness, blindness, ataxia and dementia are common findings [42, 43]. Therefore, attention has been recently focused toward

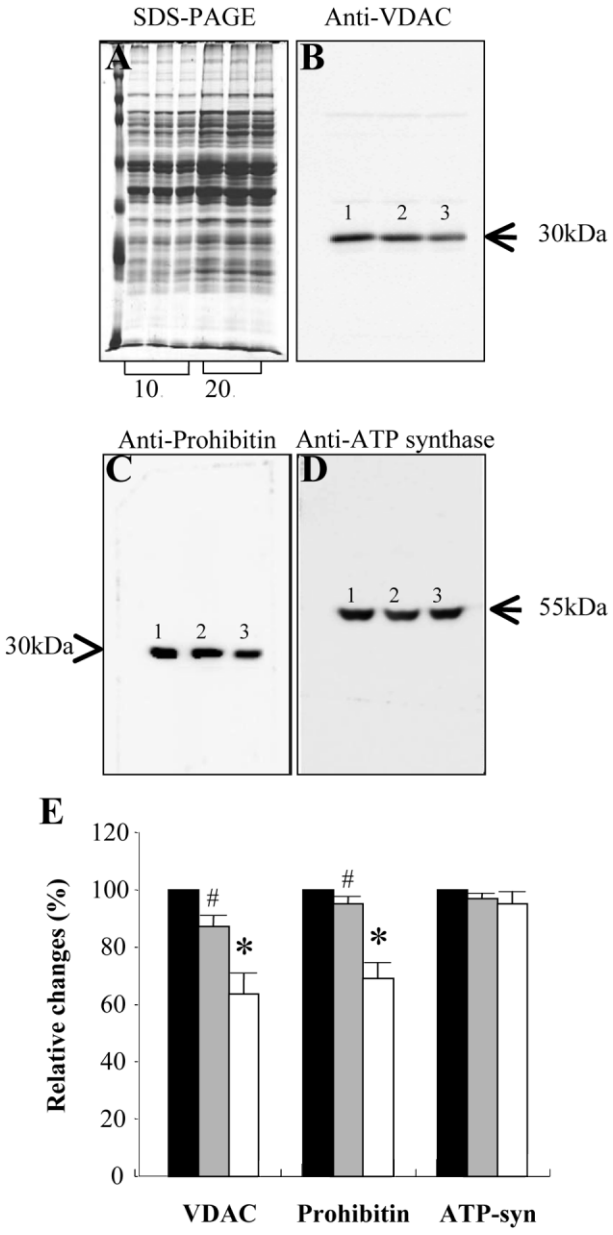

Figure 6. Western blotting analysis data of VDAC, prohibitin and ATP synthase. (A) SDS-PAGE for standardization of proteins from control, IPC and IR heart. (B) VDAC, (C) prohibitin, (D) ATP synthase (1, control; 2, IPC; 3, IR), (E), histogram of three different protein product patterns in control, IPC and IR (% to control) $^{*}p < 0.05$ *vs.* control, $^{\#}p < 0.05$ *vs.* IR.

investigation of mitochondrial biogenesis and maintenance [44]. Cardiac muscles are at most in debate regarding the vulnerability to their mitochondrial function and/or structural alterations. Functional and comparative proteomics currently afford a good reliable approach to uncover many mysteries concerning proteins expression on different cellular levels [45–48]. Several attempts have been tried on cardiac tissues to disclose mitochondrial functional proteomics in many disease conditions, *e.g.* heart mitochondria protein profiling from diabetic rats [49], chronic stressed rat heart mitochondria [50], and ischemia/reperfusion injury in rabbit myocardium [51]. However, it is still unclear whether the effect of IR on cardiac muscle has major alteration effects on mitochondrial functional proteomics. To the best of our knowledge, this study considerably resolves, for the first time, the effect of IR on mitochondrial functional proteomics in cardiac muscle, using rabbit as a model. The IR-induced mitochondrial functional proteomics alterations, in the form of expression level of different soluble proteins resolved by 2-DE, in comparison with the control ones were interpreted.

It is well known that good mitochondrial separation is a detrimental event for reliable interviewing of mitochondrial dysfunction [52–55]. This study describes the isolation and characterization of intact, functional mitochondria from the rabbit heart (Fig. 3). All mitochondrial separations were performed with a common isolation method, including gentle cell disruption via homogenization followed by crude mitochondrial separation by differential centrifugation, and finally recovery of highly purified organelles using Percoll density gradient centrifugation [56, 57]. Purity was verified using electron microscopy [27].

From the obtained data, there was general attenuation of the deleterious effect induced by IR treatment observed in IPC-treated cardiomyocytes with considerable non-significant alterations comparable with the control group. On the other hand, beside the significant elevation in LDH release and an increase in the percentage of affected infarct areas, the results showed marked alterations in level of expression of many mitochondrial proteins after IR treatment compared with the control or IPC groups. By using comparative proteomics analysis, the expression levels of 25 protein spots resolved by 2-D gel analysis were altered in IR group, 22 spots of which were successfully identified by MALDI-TOF-MS. The quantitative analysis revealed multidisciplinary proteomics remodeling process that regulates the whole mitochondrial metabolic machinery to meet with cell survival and cope against IR-induced cardiac injury. These generalized structural and functional proteomics remodeling process frames many intra-mitochondrial metabolic processes that can be addressed as follows.

3.2.2 TCA-cycle and α-keto acid dehydrogenases related proteins

In this study, two TCA-cycle related proteins were identified, namely OGDH and MDH. There expression levels were relatively decreased in IR heart. Decreased activity of these enzymes was reported in other studies during IR and other mitochondrial oxidative stress [58–61].

OGDH is a part of the OGDH complex, the mammalian OGDH enzyme complex that catalyzes oxidative decarboxylation of 2-oxoglutarate to succinyl-CoA and CO_2 [62–64]. The MDH is a 2nd candidate enzyme of the Krebs cycle that

showed a marked decrease in its expression level after IR treatment. It catalyzes the conversion of malate to oxaloacetate with production of an equivalent amount of NADH.

It is well known that in IR-induced stress cells suffer a displaced NAD/NADH ratio with overbalance of NADH in a deficit of oxygen as the final acceptor of proton in respiratory chain. Therefore, it is logical that both mitochondrial NAD-dependent MDH and OGDH have to decrease their expression level with consequent lowering of their V_{max} values. This action of down-regulation of both the Krebs cycle and oxidative phosphorylation of 2-oxoglutarate, aims at reducing the excess proton accumulation within the already stressed cells. In addition, the involvement of OGDH in the reactive oxygen species production cannot be excluded as a convenient cause to remodel its expression level during IR [65].

Spectacularly, the excess protons may safely find their draining way extra-mitochondrially via NADP-dependent intra-cytoplasmic different synthetic processes [66].

Surprisingly, in contrast to oxoglutarate, the oxidative phosphorylation of pyruvate (as an alternate α-keto acid) via the pyruvate dehydrogenase complex is seemingly not affected that much. The E1-beta subunit of pyruvate dehydrogenases complex showed a higher level of expression. It is unknown, however, whether this elevated level of expression involves the whole pyruvate dehydrogenase enzyme complex, and in turn, the rate of pyruvate turnover, or not.

3.2.3 Rsp-chain proteins

The mammalian mitochondrial NADH dehydrogenase (complex I) is the major entry point for the electron transport chain. It is the largest and most complicated respiratory complex consisting of at least 46 subunits, 7 of which are encoded by mitochondrial DNA (mtDNA) [67–69]. Deficiency in complex I function has been associated with various human diseases including neurodegenerative diseases and the aging process [70, 71].

Interestingly, the data reported a marked increase in NADH dehydrogenase complex productions after IR treatment. Recently, it has been proved to behave as a biomarker of aging. Decreasing its activity was directly related to the content of oxidation products and to the loss of physiological function in aged mice [72]. Moreover, it has been reported that mitochondrial NADH dehydrogenase activity was higher in comparatively long-lived klotho mutant mice during aging than in their wild-type counterparts [73]. Therefore, this increased level of enzyme production reported in our data can result from the compensatory mechanism that developed during short-term IR-induced stress to protect the mitochondrial compartment from the excessive level of proton production and generally induced low pH acidosis.

In contrast to NADH dehydrogenase that showed a marked increase in our data after IR induction in the heart, the Rieske iron sulfur protein, a complex III-related protein, showed a marked decrease in its expression after the same treatment as reported by 2-DE and MALDI TOF-MS. This decrease can be attributed to a mitochondrial response to slow down the rate of reactive oxygen species production generated by complex III [74].

3.2.4 Mitochondrial membrane proteins, VDAC

Recently, it has been recognized that there is a metabolic coupling between the cytosol and mitochondria, where the outer mitochondrial membrane (OMM), the boundary between these compartments, has an important function. In this crosstalk, mitochondrial Ca^{2+} homeostasis and ATP production and supply play a major role. The primary transporter of ions and metabolites across the OMM is the VDAC. The interaction of VDAC with Ca^{2+}, ATP glutamate, NADH, and different proteins was demonstrated, and these interactions may regulate OMM permeability [75]. VDAC proteins are small, abundant, pore-forming integral proteins found in the outer membrane of mitochondria and in the plasma membrane [76, 77]. The direct involvement of VDAC proteins in the loss of mitochondrial potential and cellular degeneration during IR has been reported [78]. VDAC proteins are involved in the regulation of cellular metabolism with a higher level of production reported in hypoxic neuronal cells [79]. In this study, VDAC protein expression was significantly decreased.

It is well known that the major pathway for external NADH transport across the outer membrane of many cells is constituted by VDAC [80]. However Antos *et al.* [81] concluded that in yeast uncoupled mitochondria the permeability of the highly conserved VDAC1 isoform to external NADH is probably limited when the substrate is present in higher concentrations.

These findings support the down-regulation effect induced by high NADH level on VDAC activity. Our results, however, open new speculation about the possible down-regulation of VDAC expression induced by elevated NADH during IR treatment. The limitation of VDAC expression during IR treatment may have to minimize the chance of NADH oxidation in OMM when there is a decrease in the availability of oxygen.

3.2.5 β-Oxidation-related proteins

A very interesting and fine tuning of cellular energy demand has been noticed from the data in mitochondrial control of β-oxidation enzymes during IR. This control mechanism has dual steps of modification that aims at reducing cellular demand for oxygen. These two levels of modification are mainly on levels of long chain fatty acyl CoA dehydrogenase and enoyl CoA hydratase enzymes. It is clear from the greater than 2.5-fold increase in the expressed level of long chain acyl-CoA dehydrogenase that the rate of degradation of long chain acyl CoA has to increase markedly. Transformation of fatty acyl CoA into enoyl CoA has pivotal effect on reduction of the inhibitory effect of long chain fatty acyl CoA on fatty acid synthesis. It is well known that long chain fatty

acyl CoA is the specific inhibitor of acetyl CoA carboxylase, the key regulating enzyme of fatty acid synthesis [66]. The decrease in acyl CoA level has to stimulate cellular fatty acid synthesis with concomitant incorporation of reducing equivalent via NADPH-dependent pathway. On the other hand, there is a marked decrease in the level of enoyl CoA hydratase. Accordingly, the preformed enoyl CoA has less chance to go further into β-oxidation steps. This protects the stressed cells from further reducing equivalent load as a result of 3-hydroxyacyl CoA dehydrogenase activity at the termination step of fatty acid oxidation.

Another possible regulation event that can be deduced from the present work was at the level of formation of ketone bodies. It is worth noticing, that there is a significant increase in the expression level of 3-hydroxybutyrate dehydrogenase that catalyzes the transformation of acetoacetate into β-hydroxybutyrate with consumption of 1 mole of reducing equivalent in the form of $NADH+H^+$. Thus increased expression, and consequently the V_{max} value, of the 3-hydroxybutyrate dehydrogenase enzyme may have a modulating role in phenomena of cellular protection against ischemia

3.2.6 Proliferation related proteins (structural and synthetic remodeling)

Increase of mitofilin and mtTEF in IR-treated heart can be explained as protection and recovery mechanism for the mitochondria. Mitofilin, a previously identified mitochondrial protein of unknown function, controls mitochondrial cristae morphology. Mitofilin is enriched in the narrow space between the inner boundary and the outer membranes, where it forms a homotypic interaction and assembles into a large multimeric protein complex. Down regulation of *mitofilin* in HeLa cells by using specific small interfering RNA leads to decreased cellular proliferation and increased apoptosis, suggesting abnormal mitochondrial function [82]. The higher value of mitofilin reported in IR-treated heart raises the possibility of expanding the role played by this kind of protein, from only a space filling intra-mitochondrial protein, to maintaining the normal mitochondrial morphology during stress and fighting against mitochondrial disfiguring and hence collapse of main mitochondrial function.

As a countercurrent mechanism against the accumulation of toxic compounds and many free radicals by oxidant products during generalized IR injury the mitochondria have to improve their protein synthetic machinery to rebuild and remodel their distorted polymers. This was evidenced in our data by the increase of the level of translation elongation factor protein (mtTEF). mtTEF is a GTPase that delivers amino-acylated tRNA to the ribosome during the elongation step of translation [83]. The prohibitin, on the other hand, which is a high-molecular weight complex protein found in the mitochondrial inner membrane and plays a role in the stabilization of newly synthesized subunits of mitochondrial respiratory enzymes [84, 85], showed a marked decrease in its production following IR treatment when compared with the control. This decrease in production of prohibitin during IR might be associated with the accumulation of damage from mitochondrial oxygen radicals [86].

3.2.7 Skeletal proteins

It is noteworthy that the presence of any cytoskeleton proteins reported in any of our treatment data may be a result of recovery of these proteins during separation protocol. Even though these skeletal proteins were not of mitochondrial origin and hence not part of our major scope of concern, they proved to be the primary track for mitochondrial transport and to be attached to mitochondrial membrane and regulate intracellular mitochondrial localization as well as proliferation [87, 88]. As mentioned in Section 3, the expression of actin and all other skeletal proteins increased. We suggest these increases to be caused by cellular recovery of infarct region after induction of IR in rat hearts. Interestingly, the actin alpha protein in IR-induced rat hearts showed an overexpression in comparison with control heart. This is of considerable interest because actin is a well-known anti-apoptotic protein that plays a significant role in free radical scavenging [89, 90]. Furthermore, it has been a common view that mitochondria travel on microtubule tracks in many higher eukaryotic cell types, an idea supported by numerous observations of mitochondria/microtubule relative positioning and the effects of microtubule inhibitors on mitochondrial motility [91]. Mitochondria display a variety of shapes. It has been reported that some mitochondrial shape transitions are developmentally regulated, whereas others are linked to disease or apoptosis. Mitochondrial fission depended on dynamin-related protein 1 (DRP1) and F-actin: disruption of F-actin attenuated fission and recruitment of DRP1 to the mitochondria [92].

This indicates a close relationship between mitochondrial shape and actin. Furthermore, this result suggests that the actin cytoskeleton is involved in mitochondrial fission by facilitating mitochondrial recruitment of DRP1. The role of actin as a defensive cytoskeleton candidate against stress is well-documented [93]. Mitochondrial binding to and movement along actin cables *in vitro* requires low ATP levels; at high ATP levels the interaction is disrupted [94, 88]. The IR stress can initiate mitochondrial trapping by actin. This can explain our finding of a relatively higher level of actin following IR treatment.

4 Concluding remarks

Using the comparative proteomics, the present data collectively disclose the general mitochondrial behavior in regards to functional and structural remodeling for survival during IR stress injury and counteraction behavior in normal control or IPC treatments. This proteomic analysis of mitochondrial proteins in control, IPC- and IR-treated rabbit car-

diomyocytes provided an effective approach for elucidating the molecular mechanisms of IR-induced cardiovascular injury and protection effect of IPC. Twenty-five protein spots with different abundance were found by 2-DE, of which twenty-two differentially expressed proteins were identified by MALDI-TOF MS. These identified proteins in IR-induced mitochondrial injury were confirmed by Western blot analysis and discussed. The successful use of multiple techniques, including 2-DE and MALDI-TOF-MS, demonstrates that proteomic analysis provides appropriate means for identifying cardiac biomarkers as a measure for detecting ischemia-induced cardiac injury.

This work was supported by Grants R05-2003-000-00413-0 and R05-2004-000-00905-0 of the Korea Science and Engineering Foundation, the Korea Research Foundation Grant funded by the Korean Gouvernment (MOEHRD) (KRF-2002-E00076, KRF-2002-042-E00006, KRF-2003-015-E00025, KRF-2005-210-E00003 and KRF-2005-211-E00006, KRF-2005-037-E00002), the Research Project on the Production of Bio-organs, Ministry of Agriculture and Forestry, Republic of Korea, and a grant from the Ministry of Commerce, Industry and Energy (MOCIE) and Korea Institute of Industrial Technology Evaluation & PLanning (ITEP) through the Biohealth Products Research Center (BPRC) of Inje University.

5 References

[1] Carroll, R., Yellon, D. M., *Int. J. Cardiol.* 1999, *68*, S93–S101.

[2] Miller, D. L., Van Winkle, D. M., *Cardiovasc. Res.* 1999, *42*, 680–684.

[3] Braunwald, E., Kloner, R. A., *J. Clin. Invest.* 1985, *76*, 1713–1719.

[4] McCord, J. M., Roy, R. S., Schaffer, S. W., *Adv. Myocardiol.* 1985, *5*, 183–189.

[5] Gottlieb, R. A., Burleson, K. O., Kloner, R. A., Rodriguez, E. *et al.*, *J. Clin. Invest.* 1994, *94*, 1621–1628.

[6] Bialik, S., Cryns, V. L., Drincic, A., Miyata, S. *et al.*, *Circ. Res.* 1999, *85*, 403–414.

[7] Han, J., Kim, N., Joo, H., Kim, E., *Am. J. Physiol. Heart Circ. Physiol.* 2002, *283*, H13–H21.

[8] Han, J., Kim, N., Park, J., Seog, D. H. *et al.*, *J. Biochem.* 2002, *131*, 721–727.

[9] Murry, C. E., Jennings, R. B., Reimer, K. A., *Circulation* 1986, *74*, 1124–1136.

[10] Fabrizo, T., Filippo, C., Ligo, C., Pier, A., *Circulation* 1999, *100*, 559–563.

[11] Riksen, N. P., Smits, P., Rongen, G. A., *Neth. J. Med.* 2004, *62*, 353–363.

[12] Martin, C., *Biochem. J.*, 1999, *341*, 233–249.

[13] Schwertz, H., Langin, T., Platsch, H., Richert, J. *et al.*, *Proteomics* 2002, *2*, 988–995.

[14] Hirano, M., Davidson, M., DiMauro, S., *Curr. Opin. Cardiol.* 2001, *16*, 201–210.

[15] Beal, M. F., Howell, N., Bodis Wallner, I., (Eds.), *Mitochondria and Free Radicals in Neurodegenerative Diseases*, Wiley-Liss, New York 1997.

[16] Yarian, C. S., Rebrin, I., Sohal, R. S., *Biochem. Biophys. Res. Commun.* 2005, *330*, 151–156.

[17] Jugdutt, B. I., *Am. J. Physiol.* 1997, *272*, H1205–H1211.

[18] Lee, Y., Kim, N., Kim, H., Joo, H. *et al.*, *Korean J. Physiol. Pharmacol.* 2004, *4*, 207–212.

[19] Cuong, D., Kim, N., Cho, H., Kim, E. *et al.*, *Korean J. Physiol. Pharmacol.* 2004, *2*, 95–100.

[20] Cleveland, J. C., Wollmering, M. M., Meldrum, D. R., Rowland, R. T. *et al.*, *Am. J. Physiol. Heart Circ. Physiol.* 1996, *271*, H1786–H1794.

[21] Roscoe, A. K., Christensen, J. D., Lynch, C., *Anesthesiology* 2000, *92*, 1692–1701.

[22] Mullenheim, J., Frassdorf, J., Preckel, B., Thamer, V. *et al.*, *Anesthesiology* 2001, *94*, 630–636.

[23] Johnson, G., Tsao, P. B. S., Lefer, A. M., *Am. Heart J.* 1990, *119*, 530–538.

[24] Fishbein, M. C., Meerbaum, S., Rit, J., *Am. Heart J.* 1981, *101*, 593–600.

[25] Han, J., Kim, N., Joo, H., Kim, E., *Am. J. Physiol. Heart Circ. Physiol.* 2002, *283*, H13–H21.

[26] Ulrich, M., Roland, L., *Encyclopedia of Life Sciences*, 2002, pp. 1–8.

[27] Rajapakse, N., Shimizu, K., Payne, M., Busija, D., *Brain Res. Brain Res. Protoc.* 2001, *8*, 176–183.

[28] Berkelman, T., Stenstedt, T., *2-D Electrophoresis, Using Immobilized pH gradients, Principles and Methods*, Amersham Pharmacia Biotech, Uppsala, Sweden 1998, pp. 14–36.

[29] Rosenfeld, J., Capdevielle, J., Guillemot, J. C., Ferrara, P., *Anal. Biochem.* 1992, *203*, 173–179.

[30] Moyle, G., *Antivir. Ther.* 2005, *10*, M47–M52.

[31] Newman, N. J., *Am. J. Ophthalmol.* 2005, *140*, 517–523.

[32] Kato, T., Kuratomi, G., Kato, N., *Drugs Today* 2005, *41*, 335–344.

[33] Liu, J., Ames, B. N., *Nutr. Neurosci.* 2005, *8*, 67–89.

[34] Manfredi, G., Xu, Z., *Mitochondrion* 2005, *5*, 77–87.

[35] Sarnat, H. B., Marin-Garcia, J., *Can. J. Neurol. Sci.* 2005, *32*, 152–166.

[36] Yan, S. D., Stern, D. M., *Int. J. Exp. Pathol.* 2005, *86*, 161–171.

[37] Arpa-Gutierrez, F. J., Cruz-Martinez, A., Campos-Gonzalez, Y., Gutierrez-Molina, M. *et al.*, *Rev. Neurol.* 2005, *41*, 449–454.

[38] Stanley, W. C., Recchia, F. A., Lopaschuk, G. D., *Physiol. Rev.* 2005, *85*,1093–1129.

[39] Calabrese, V., Lodi, R., Tonon, C., D'Agata, V., *et al.*, *J. Neurol. Sci.* 2005, *233*,145–162.

[40] Puddu, P., Puddu, G. M., Galletti, L., Cravero, E. *et al.*, *Cardiology* 2005, *103*, 137–141.

[41] Dimauro, S., Mancuso, M., Naini, A., Ann. N. Y., *Acad. Sci.* 2004, *1011*, 232–245.

[42] Schapira, A. H., *Biochim. Biophys. Acta* 1998, *1366*, 225–233.

[43] Truong, D. D., Harding, A. E., Scaravilli, F., Smith, S. J. *et al.*, *Mov. Disord.* 1990, *5*, 109–117.

[44] Attardi, G. M., Chomyn, A., *Methods Enzymol.*, Academic Press, San Diego 1995, p. *260*.

[45] Topanurak, S., Sinchaikul, S., Sookkheo, B., Phutrakul, S. *et al.*, *Proteomics* 2005, *Epub*.

[46] Monti, M., Orru, S., Pagnozzi, D., Pucci, P., *Biosci. Rep.* 2005, *25*, 45–56.

[47] Huang, C. M., Xu, H., Wang, C. C., Elmets, C. A., *Expert Rev. Proteomics* 2005, *2*, 809–820.

[48] Matsumoto, M., Hatakeyama, S., Oyamada, K., Oda, Y. *et al.*, *Proteomic*, 2005, *Epub.*

[49] Illarion, V. T., Ferid, M., *J. Biol. Chem.*, 2003, *278*, 35844–35849.

[50] Liu, X. H., Qian, L. J., Gong, J. B., Shen, J. *et al.*, *Proteomics* 2004, *4*, 3167–3176.

[51] White, M. Y., Cordwell, S. J., McCarron, H. C., Prasan, A. M. *et al.*, *Proteomics* 2005, *5*, 1395–1410.

[52] Cao, J., Zheng, C. D., Zhang, G. X., Zhang, Y. J. *et al.*, *Chin. Med. J.* 2005, *118*, 505–507.

[53] Zhang, Y. M., Zhao, D. H., Sheng, B. H., *Yao Xue Xue Bao* 1991, *26*, 144–146.

[54] Chaiswing, L., Cole, M. P., St. Clair, D. K., Ittarat, W. *et al.*, *Toxicol. Pathol.* 2004, *32*, 536–547.

[55] Lundberg, K. C., Szweda, L. I., *Arch. Biochem. Biophys.* 2004, *432*, 50–57.

[56] Redon, A., Masmoudi, A., *J. Neurosci. Methods* 1985, *14*, 41–51.

[57] Sims, N. R., *J. Neurochem.* 1990, *55*, 698–707.

[58] Zanozdra, M. M., Khmelevs'kii, IuV., *Ukr. Biokhim. Zh.* 1977, *49*, 51–54.

[59] Gibson, G. E., Blass, J. P., Beal, M. F., Bunik, V., *Mol. Neurobiol.* 2005, *31*, 43–63.

[60] Huang, H. M., Ou, H. C., Xu, H., Chen, H. L. *et al.*, *J. Neurosci. Res.* 2003. *74*, 309–317.

[61] Park, L. C., Zhang, H., Sheu, K. F., Calingasan, N. Y. *et al.*, *J. Neurochem.* 1999, *72*, 1948–1958.

[62] Reed, L. J., *Acc. Chem. Res.* 1974, *7*, 40–46.

[63] Koike, M., Koike, K., *Adv. Biophys.* 1976, *9*, 182–227.

[64] Yeaman, S. J., *Biochem. J.* 1989, *257*, 625–632.

[65] de Grey, A. D., *Rejuvenation Res.* 2005, *8*, 13–17.

[66] Nellon, D. L., Cox, M. M., *Lehniger Principles of Biochemistry*, Worth Publishers, New York 2000, *3rd ed.*, pp. 770–817.

[67] Hirst, J., Carroll, J., Fearnley, I. M., Shannon, R. J. *et al.*, *Biochim. Biophys. Acta* 2003, *1604*, 135–150.

[68] Wikström, M., *FEBS Lett.* 1984, *169*, 300–304.

[69] Galkin, A. S., Grivennikova, V. G., Vinogradov, A., *FEBS Lett.* 1999, *451*, 157–161.

[70] Van den Heuvel, L., Smeitink, J., *Bioessays* 2001, *23*, 518–525.

[71] Singer, T. P., Ramsay, R. R., Ackrell, B. A., *Biochim. Biophys. Acta* 1995, *24*, 211–219.

[72] Navarro, A., *Mol. Aspects Med.* 2004, *25*, 37–48.

[73] Sato, I., Miyado, M., Sunohara, M., Okajimas, F., *Anat. Jpn.* 2005, *82*, 49–56.

[74] O'Rourke, B., Cortassa, S., Aon M., *Physiology* 2005, *20*, 303–315.

[75] Shoshan-Barmatz, V., Israelson, A., *J. Membr. Biol.* 2005, *204*, 57–66.

[76] Yu, W. H., Wolfgang, W., Forte, M., *J. Biol. Chem.* 1995, *270*, 13998–14006.

[77] Bathori, G., Parolini, I., Tombola, F., Szabo, I. *et al.*, *J. Biol. Chem.* 1999, *274*, 29607–29612.

[78] Perez-Velazquez, J. L., Frantseva, M. V., Huzar, D. V., Carlen, P. L., *Neuroscience* 2000, *97*, 363–369.

[79] Shinohara, Y., Ishida, T., Hino, M., Yamazaki, N. *et al.*, *Eur. J. Biochem.* 2000, *267*, 6067–6673.

[80] Lee, A. C., Xu, X., Blachly-Dyson, E., Forte, M. *et al.*, *J. Membr. Biol.* 1998, *161*, 173–181.

[81] Antos, N., Stobienia, O., Budzinska, M., Kmita, H., *J. Bioenerg. Biomembr.* 2001, *33*, 119–126.

[82] John, G. B., Shang, Y., Li, L., Renken, C. *et al.*, *Mol. Biol. Cell* 2005, *16*, 1543–1554.

[83] Chiron, S., Suleau, A., Bonnefoy, N., *Genetic.* 2005, *169*, 1891–1901.

[84] Nijtmans, L. G., de Jong, L., Artal Sanz, M., Coates, P. J. *et al.*, *EMBO J.* 2000, *19*, 2444–2451.

[85] Coates, P. J., Jamieson, D. J., Smart, K., Prescott, A. R. *et al.*, *Curr. Biol.* 1997, *7*, 607–610.

[86] Back, J. W., Sanz, M. A., De Jong, L., De Koning, L. J. *et al.*, *Protein Sci.* 2002, *11*, 2471–2478.

[87] Sturmer, K., Baumann, O., Walz, B., *J. Cell Sci.* 1995, *108*, 2273–2283.

[88] Simon, V. R., Swayne, T. C., Pon, L. A., *J. Cell. Biol.* 1995, *130*, 345–354.

[89] Gourlay, C. W., Ayscough, K. R., *Nat. Rev. Mol. Cell Biol.* 2005, *6*, 583–589.

[90] Touyz, R. M., Yao, G., Schiffrin, E. L., *Can. J. Physiol. Pharmacol.* 2005, *83*, 91–97.

[91] Hales, K. G., *Mitochondrion* 2004, *4*, 285–308.

[92] De Vos, K. J., Allan, V.J., Grierson, A.J., Sheetz, M. P., *Curr. Biol.* 2005, *15*, 678–683.

[93] Condrescu, M., Reeves, J. P., *Am. J. Physiol. Cell Physiol.* 2005, *Epub.*

[94] Lazzarino, D. A., Boldogh, I., Smith, M. G., Rosand, J. *et al.*, *Mol. Biol. Cell.* 1994, *5*, 807–818.

